Pure single-photon emission from an InGaN/GaN quantum dot

Cite as: APL Mater. 9, 061106 (2021); doi: 10.1063/5.0049488
Submitted: 5 March 2021 • Accepted: 2 June 2021 •
Published Online: 14 June 2021

M. J. Holmes,[1,2,a] T. Zhu,[3] F. C.-P. Massabuau,[3,4] J. Jarman,[3] R. A. Oliver,[3] and Y. Arakawa[2]

AFFILIATIONS

[1] Institute of Industrial Science, The University of Tokyo, 4-6-1 Komaba, Meguro-ku, Tokyo 153-8505, Japan
[2] Institute for Nano Quantum Information Electronics, The University of Tokyo, 4-6-1 Komaba, Meguro-ku, Tokyo 153-8505, Japan
[3] Department of Materials Science and Metallurgy, The University of Cambridge, 27 Charles Babbage Road, Cambridge CB3 0FS, United Kingdom
[4] Department of Physics, SUPA, University of Strathclyde, Glasgow G4 0NG, United Kingdom

[a] **Author to whom correspondence should be addressed:** holmes@iis.u-tokyo.ac.jp

ABSTRACT

Single-photon emitters with high degrees of purity are required for photonic-based quantum technologies. InGaN/GaN quantum dots are promising candidates for the development of single-photon emitters but have typically exhibited emission with insufficient purity. Here, pulsed single-photon emission with high purity is measured from an InGaN quantum dot. A raw $g^{(2)}(0)$ value of 0.043 ± 0.009 with no corrections whatsoever is achieved under quasi-resonant pulsed excitation. Such a low value is, in principle, sufficient for use in quantum key distribution systems.

INTRODUCTION

Semiconductor quantum dots (QDs) are being developed from a wide variety of materials for the realization of single-photon emitters for quantum photonic applications.[1,2] III-nitride QDs are an interesting prospect for such technologies as they can allow for the generation of single photons from the near UV to the infrared,[3–5] are capable of operation at high temperature[6–9] (or at temperatures accessible with thermoelectric cooling[10]), and can be developed for emission with deterministic polarization.[10] This wide range of tunable emission can also potentially allow for the development of tailored emitters for different applications, such as interfacing with various quantum memories developed from ions with specific transition energies. Although the development of quantum emitters using III-nitrides is still being researched heavily in academic laboratories, the III-nitride material system itself benefits from a well-developed industrial infrastructure due to its widespread use in solid-state lighting and power electronics applications. InGaN/GaN and GaN/AlGaN QDs have therefore been the subject of intense research interest, but several issues pertaining to emitter performance must still be overcome before realistically usable devices can be developed. One such major issue is the emission purity, characterized by the value of the second order intensity autocorrelation at zero time delay: $g^{(2)}(0)$. While experimentally measured $g^{(2)}(0)$ values lower than 0.5 are sufficient to claim the presence of a single quantum emitter,[11] $g^{(2)}(0)$ values lower than 0.1 are required for even the most technologically forgiving application: quantum key distribution (QKD).[12] High degrees of purity have been realized from a wide range of QD-based emitters, including InAs/InP,[13,14] InGaAs/GaAlAs,[15–17] CdSe/ZnSe,[18] and GaN/AlGaN[19] QDs. However, even the purest single-photon-emitting InGaN/GaN QDs developed to date exhibit $g^{(2)}(0)$ values greater than 0.1.[7,20–24] This is due to insufficient isolation of the emitters, often due to spectral overlap between the photons emitted from the QD and the background emission from the surrounding quantum well that forms during sample fabrication. Additional effects, such as spectral diffusion/wandering, act to broaden the emission linewidths,[25] exacerbating the difficulties in achieving a high degree of spectral isolation. It is of crucial importance to develop high-purity InGaN/GaN single-photon emitters as it is the addition of indium that, in principle, allows for significant wavelength tunability into the visible and possibly IR. Here, we report the successful generation of single photons with a high degree of purity from an isolated InGaN/GaN QD, showing that the

material system can indeed be used for high quality single-photon emission.

EXPERIMENT

The InGaN/GaN QDs used in this study were grown on a c-plane sapphire substrate using metal–organic vapor phase epitaxy in a Thomas Swan close-coupled showerhead reactor using a modified droplet epitaxy method and are formed within a 200 nm thick intrinsic GaN layer. This approach leads to the formation of QDs along with a fragmented quantum well,[26,27] which has implications on the optical properties as discussed below. The density of QDs in the samples used here is ~3×10^8 cm^{-2}: sufficiently low for the optical measurement of isolated individual structures. The QD active region is sandwiched between two planar porous distributed Bragg reflectors,[20,28,29] and the sample is processed into micro-pillar structures (~1 μm in diameter, using silica microspheres as an etch mask) to enhance the optical extraction efficiency (although we note that we observe no cavity-specific effects such as Purcell enhancement from the sample). Figure 1 shows a high-angle annular dark field scanning transmission electron microscope (HAADF-STEM) image and a corresponding energy dispersive x-ray (EDX) spectroscopy map of the QD layer, measured using the sequential plan-view method.[30] Due to the droplet epitaxy growth mode, the QDs form with a high compositional contrast to the surrounding material, which is expected to lead to strong quantum confinement and QD emission with little-to-no background contamination from the surrounding material. Moreover, further suppression of any emission background can be expected due to the nature of the fractured quantum well, which, combined with the proximity of the micro-pillar side walls, will promote non-radiative recombination from carriers that are not confined in the QDs.

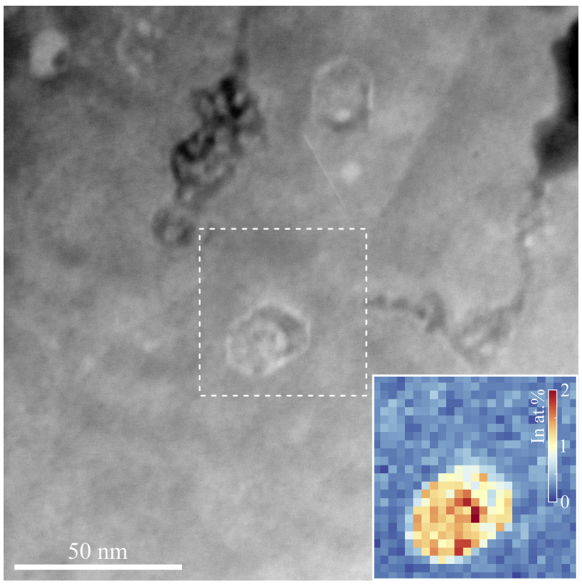

FIG. 1. Plan-view HAADF-STEM image of the QD layer on a fractured quantum well used in the study. The inset shows a magnified EDX image of the center region, where a QD with a high compositional contrast to the surrounding material can be seen. The lateral size of the QD is on the order of 20 nm. Note that the value of the indium atomic percentage presented in the figure inset is measured as a projection through the surrounding barrier material and therefore does not accurately represent the absolute value of the material in the QD.

Optical excitation of the dots was performed using a pulsed laser (the second harmonic of a Ti:sapphire laser at 375 nm, operating at 80 MHz). The excitation wavelength was chosen to suppress excitation of carriers into the surrounding GaN material (which has a bandgap of 3.5 eV) and therefore provide quasi-resonant excitation directly into the continuum states of the QDs (or parts of the surrounding fragmented quantum well). Excitation was performed through a 50× objective lens (NA 0.65) using a laser spot size of ~1 μm. The sample was held at a temperature of 9 K in a closed-cycle helium cryocooler (AttoDRY 800), and the emission was collected using the same objective lens and directed to a 30 cm spectrometer with 1200 l mm^{-1} grating and a CCD detector. A Hanbury Brown and Twiss (HBT) setup was used at one exit slit of the spectrometer to measure the second order autocorrelation and determine the purity of the emitted photons. The HBT consisted of a 50/50 beam splitter and two photomultiplier tubes (PMTs) connected to timing electronics (Picoharp 300) to measure the time delay between detection events.

Bright and stable emission from a selected QD was observed at a wavelength of 435 nm (see Fig. 2). The emission spectrum consists of a sharp peak with a linewidth (FWHM) of 2.2 meV and a low energy sideband due to phonon-assisted recombination. Although this dot emits at 435 nm, we note that we observe emission peaks from different QDs with wavelengths varying from 420 to 480 nm (due to the strong piezoelectric fields in III-nitride materials, the emission energy can vary strongly for even small differences in the QD size[31–33]). The particularly low degree of contaminating background emission for this emitter, corresponding to ~2.5% of the total integrated intensity, makes it an ideal candidate for investigation as a high-purity single-photon emitter (the background emission varies from emitter to emitter and is likely related to the emission of the fractured InGaN quantum well and possibly some other weakly excited QDs). The right figure insets show the power dependence of the emission linewidth and intensity (corresponding to the combined photon count rates on the two PMT detectors). The emission intensity exhibits a linear increase with excitation power before saturation at a detected-count rate of 4.0×10^4 cps. The emission lifetime (shown in the left figure inset) was measured to be 640 ps using time resolved micro-photoluminescence under excitation at the same conditions, suggesting that the QD may be relatively small with a high degree of electron–hole wavefunction overlap (see the left figure inset). The saturated count rate on the PMTs of 4.0×10^4 cps corresponds to a photon flux of 8.3 MHz into the front element of the NA 0.65 objective lens when accounting for the throughput of the experimental system (see the section titled Methods). Under excitation conditions of 80 MHz (and under the assumption of 100% internal quantum efficiency), this corresponds to a collection efficiency of ~10.4% into the surface of the objective lens.

The single-photon nature of the emission was confirmed via measurements of the second order intensity autocorrelation, $g^{(2)}(\tau)$, as a function of excitation power. The data for excitation at a power of 0.2 μW (excitation power measured just before the objective lens) are shown in Fig. 3. Clear antibunching is observed via the absence of a peak at time delay $\tau = 0$. Analysis of the

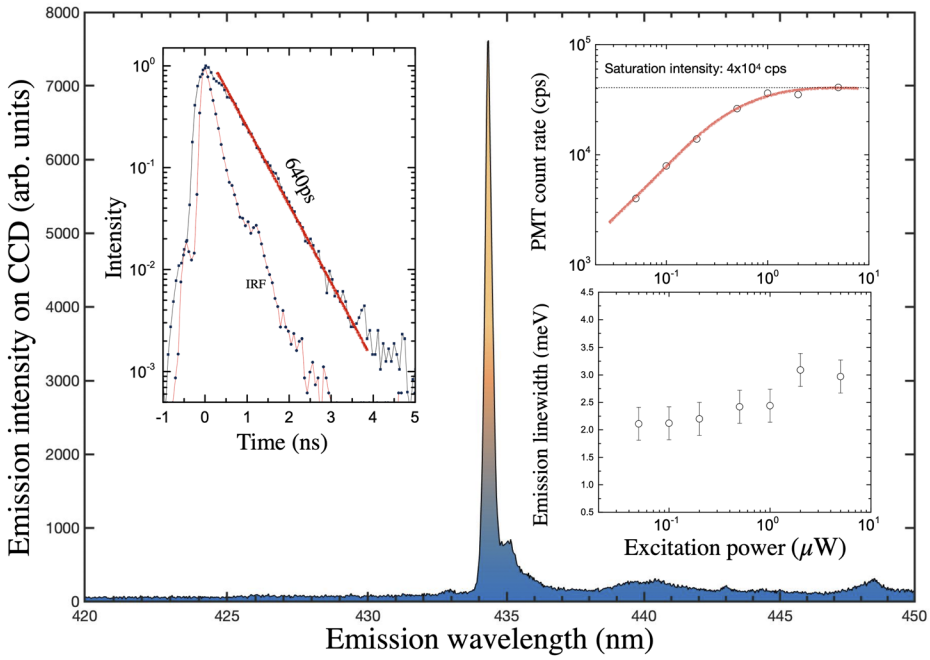

FIG. 2. Emission spectrum of the studied emitter measured at an excitation power of 0.2 μW (excitation power measured just before the objective lens). The left figure inset shows a measurement of the emission lifetime at the same excitation power, and the right upper inset shows the saturation curve of the photon count rate on the PMT detectors (emission intensity) as a function of excitation power (the solid line is a guide to the eye). The right lower inset shows the power dependence of the emission linewidth.

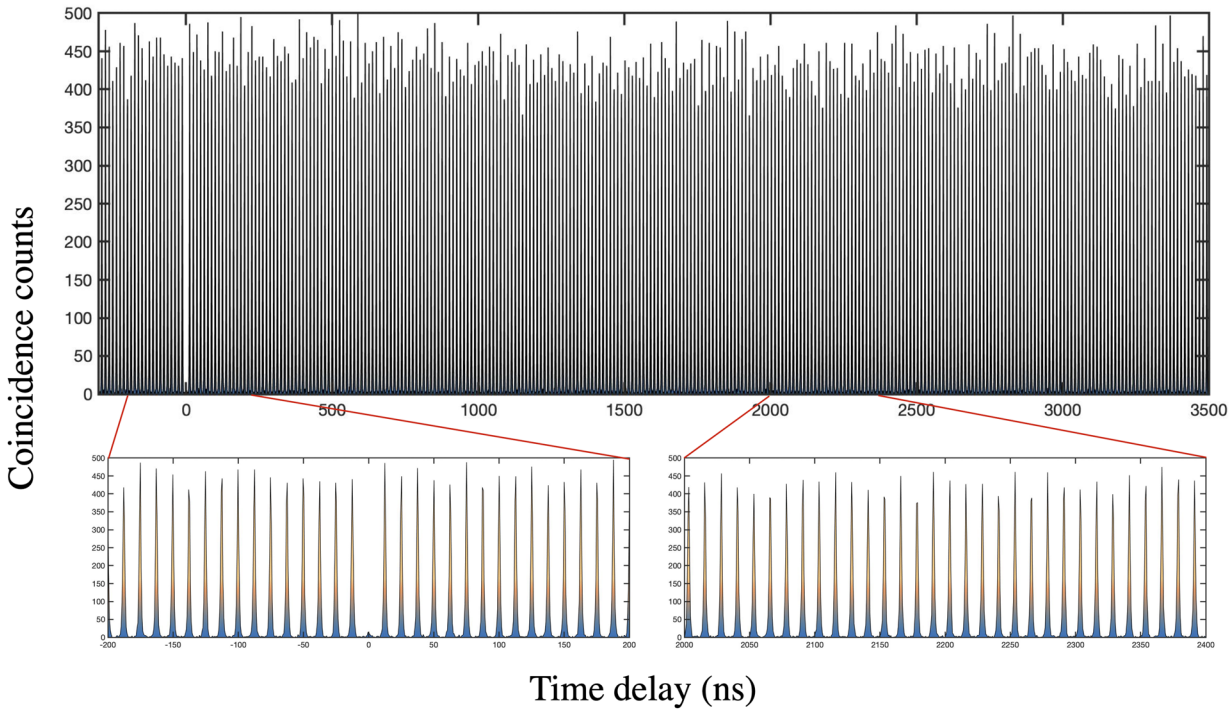

FIG. 3. Autocorrelation for the emission measured at an excitation power of 0.2 μW showing a strong degree of antibunching at time delay zero. The plots at the bottom show zoomed-in regions around time delay zero and at longer delay. The $g^{(2)}(0)$ value, calculated as the ratio of the zero-delay peak intensity to the average side-peak intensity, is 0.043 ± 0.009.

$g^{(2)}(0)$ value (evaluated as the ratio of the integrated counts in the central peak to the average counts in the side peaks) reveals a value of 0.043 ± 0.009, clearly showing the high degree of single-photon emission purity. The excitation power dependence of $g^{(2)}(0)$ is presented in Fig. 4. Purer single-photon emission is achieved at lower excitation powers, with a slight degradation in purity as the excitation power is increased. This is likely due to a combination of higher impact of background contamination for excitation powers above the QD saturation power and a higher likelihood of fast re-excitation–emission processes due to the not-strictly resonant excitation.[15] However, for excitation powers below the saturation power, it is clear that $g^{(2)}(0)$ can be maintained below 0.1. As the power is lowered further, the measured $g^{(2)}(0)$ values level off at a value of ~0.05. The $g^{(2)}(0)$ values presented here have been extracted from the raw data (without any corrections applied whatsoever) and are therefore representative of the true extent of the purity to which the photons can be extracted, filtered, and ultimately delivered to any downstream optical system. While these data represent the purest emission that we could observe, we note that other emission peaks from the sample exhibited $g^{(2)}(0)$ values ranging from 0.1 to 0.46, depending on the amount of background emission.

Finally, we discuss the linewidth of the emission, which at ~2.2 meV is broadened significantly beyond the transform-limited value of the 640 ps emission lifetime. Typical linewidth-broadening mechanisms include phonon interactions[34,35] and fast spectral diffusion induced by fluctuating charge in the emitters' local environment (which interacts with the charge confined in the QD to cause a temporally varying shift in the QD emission energy).[25,36,37] Unfortunately, c-plane III-nitride QDs tend to suffer strongly from such environmental interactions[25,38] due to a combination of their large internal electric fields and a high density of defects in typically grown material. The phonon interactions can lead to strong sidebands,[38] and fast spectral diffusion can occur on time scales ranging down to a few tens of ns,[28,39] resulting in linewidths that appear

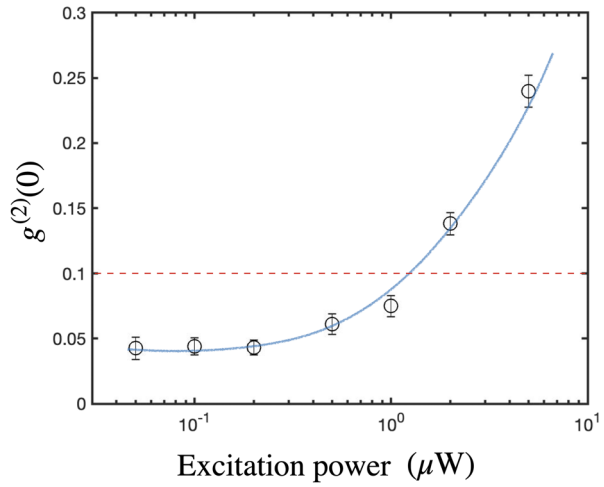

FIG. 4. Excitation power dependence of the $g^{(2)}(0)$ value. $g^{(2)}(0) < 0.1$ can be maintained for excitation powers lower than 1 μW (the solid line is a guide to the eye).

to be broadened up to several meV when measured using typical CCD detectors that cannot resolve such fast processes. It is possible that these interactions may be suppressed in the future by changing to a non/semi-polar growth plane,[10] by using III-nitrides with zinc-blende structure,[40] or by the growth of material with significantly reduced defect density.[19] Here, we evaluate the characteristic spectral diffusion time scale of the emitter discussed in this paper by performing a $g^{(2)}(\tau)$ measurement under strict spectral filtering using a bandpass filter, which is narrower (controlled by the exit slit of the spectrometer) than the diffusion-limited linewidth.[41,42] Under such experimental conditions, the fluctuations in the charge in the local environment of the QD cause the QD emission energy to randomly shift in and out of the spectral measurement window, leading to a bunching in the intensity autocorrelation with a time scale corresponding to that of the environmental charge fluctuations [as shown schematically in Fig. 5(a)]. This can be simply explained via the following: The detection of a photon implies that the QD emission energy at the time of emission was within the measurement spectral window, and it is therefore statistically more likely to detect a second photon within a short time period as opposed to on a longer time scale when the QD emission energy may have drifted out of the measurement window. Hence, the intensity autocorrelation becomes larger for small but finite time differences.

For the experiments here, we used an exit slit corresponding to a bandpass of ~1 meV: about half of the emission linewidth (narrowing the exit slit results in greater visibility of the bunching but significantly increases the integration time required for the experiment). The autocorrelation measured at an excitation power of 0.2 μW is shown on an extended scale in Fig. 5(b) from which the diffusion-induced bunching time scale is extracted (via an exponential decay fitting to the integrated peak intensity) to have a characteristic time scale of ~897 ± 43 ns. Note that the bunching does not appear in Fig. 3, which was acquired using a full-width measurement of the same emitter under the same excitation conditions. The power dependence of the spectral diffusion time scale is presented in Fig. 5(c), where the increased excitation is shown to rapidly increase the rate of spectral diffusion such that the diffusion time scale is reduced to 265 ns at the saturation power of the dot. This is likely due to the increased density of carriers excited in the region around the QD (and possibly in the surrounding GaN via the excitation to/from mid-gap trap states). Nevertheless, it is promising that such long diffusion times can be measured from these QDs as longer diffusion times will allow for a larger number of photons to be emitted between fluctuations in the QD emission energy, which is one important parameter toward the generation of stable sources of indistinguishable photons.[43]

In summary, we have realized a bright and high-purity single-photon source based on an InGaN/GaN QD in a fractured quantum well. $g^{(2)}(0)$ values <0.1 were achievable even at the saturation power of the dot, whereby the photon flux into the NA 0.65 objective lens was on the order of 8.3 MHz. Spectral diffusion due to fluctuations in the electronic environment (occurring on time scales of a few 100 ns) currently dominates the emission linewidth. Finally, we note that, due to the short lifetime of the emitter (~640 ps), the photon collection rate could, in principle, be increased trivially by using a higher excitation rate.

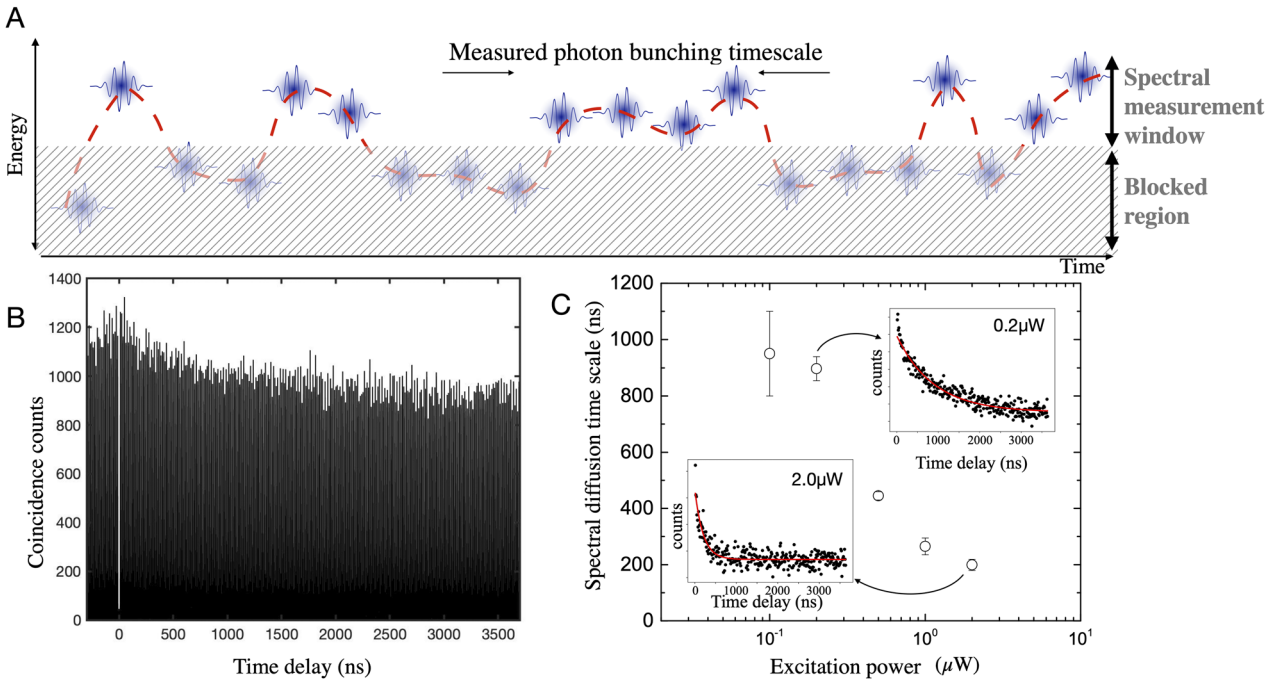

FIG. 5. Spectral diffusion time scale measurements. (a) Simplified explanation of the spectral diffusion time scale measurement, whereby a filter is used to block half of the emission that fluctuates in time. The narrow measurement window leads to an additional bunching in the autocorrelation data due to the fluctuation of the emission in and out of the measurement window. (b) Spectral diffusion measurement at an excitation power of 0.2 μW, revealing a bunching with a characteristic time scale of 897 ± 43 ns. (c) Power dependence of the measured spectral diffusion time scale (the figure insets show the fitting used to extract the spectral diffusion time scales).

METHODS

The brightness of the emitter is evaluated as the emission rate into the first element of the objective lens (MITSUTOYO M Plan Apo NUV HR 50×) and is calculated by calibrating the count rates on the PMTs with the efficiency of the optical setup (objective throughput: 77%, dichroic mirror 95%, directing optics including spectrometer and focusing lenses: 2.4%, and PMT efficiency: 27.6%). This efficiency was calculated using spec sheet values at 430 nm where possible, but the throughput of the directing optics and spectrometer was measured using a reflected laser beam at 402 nm that had been focused onto the sample and recollimated by the objective lens (although no significant deviations between 400 and 435 nm are expected).

The spectral resolution of the spectrometer is ~900 μeV and the temporal resolution of the PMT detector including electronic jitter [as shown in the instrument response function (IRF) in Fig. 1 is 266 ps]. The temporal resolution of the HBT setup including both PMTs is 477 ps (measured using the autocorrelation of a femtosecond laser).

ACKNOWLEDGMENTS

This work was supported by the JSPS KAKENHI (Project No. 19K15039); the KAKENHI Grant-in-Aid for Specially Promoted Research (Grant No. 15H05700); the TAKUETSU program of the Ministry of Education, Culture, Sports, Science and Technology, Japan; and the UK Engineering and Physical Sciences Research Council (Grant No. EP/M011682/1).

DATA AVAILABILITY

The data that support the findings of this study are available from the corresponding author upon reasonable request.

REFERENCES

[1] P. Senellart, G. Solomon, and A. White, Nat. Nanotechnol. **12**, 1026 (2017).
[2] Y. Arakawa and M. J. Holmes, Appl. Phys. Rev. **7**, 021309 (2020).
[3] S. Tomić, J. Pal, M. A. Migliorato, R. J. Young, and N. Vukmirović, ACS Photonics **2**, 958 (2015).
[4] T. Zhu and R. A. Oliver, Europhys. Lett. **113**, 38001 (2016).
[5] M. J. Holmes, M. Arita, and Y. Arakawa, Semicond. Sci. Technol. **34**, 033001 (2019).
[6] M. J. Holmes, K. Choi, S. Kako, M. Arita, and Y. Arakawa, Nano Lett. **14**, 982 (2014).
[7] S. Deshpande, T. Frost, A. Hazari, and P. Bhattacharya, Appl. Phys. Lett. **105**, 141109 (2014).
[8] M. J. Holmes, S. Kako, K. Choi, M. Arita, and Y. Arakawa, ACS Photonics **3**, 543 (2016).
[9] S. Tamariz, G. Callsen, J. Stachurski, K. Shojiki, R. Butté, and N. Grandjean, ACS Photonics **7**, 1515 (2020).
[10] T. Wang, T. J. Puchtler, T. Zhu, J. C. Jarman, L. P. Nuttall, R. A. Oliver, and R. A. Taylor, Nanoscale **9**, 9421 (2017).
[11] S. Buckley, K. Rivoire, and J. Vučković, Rep. Prog. Phys. **75**, 126503 (2012).

[12]I. Aharonovich, D. Englund, and M. Toth, Nat. Photonics **10**, 631 (2016).
[13]T. Miyazawa, K. Takemoto, Y. Nambu, S. Miki, T. Yamashita, H. Terai, M. Fujiwara, M. Sasaki, Y. Sakuma, M. Takatsu, T. Yamamoto, and Y. Arakawa, Appl. Phys. Lett. **109**, 132106 (2016).
[14]A. Musiał, P. Holewa, P. Wyborski, M. Syperek, A. Kors, J. P. Reithmaier, G. Sęk, and M. Benyoucef, Adv. Quantum Technol. **3**, 1900082 (2020).
[15]L. Schweickert, K. D. Jöns, K. D. Zeuner, S. F. Covre da Silva, H. Huang, T. Lettner, M. Reindl, J. Zichi, R. Trotta, A. Rastelli, and V. Zwiller, Appl. Phys. Lett. **112**, 093106 (2018).
[16]L. Hanschke, K. A. Fischer, S. Appel, D. Lukin, J. Wierzbowski, S. Sun, R. Trivedi, J. Vučković, J. J. Finley, and K. Müller, npj Quantum Inf. **4**, 43 (2018).
[17]H. Wang, H. Hu, T.-H. Chung, J. Qin, X. Yang, J.-P. Li, R.-Z. Liu, H.-S. Zhong, Y.-M. He, X. Ding, Y.-H. Deng, Q. Dai, Y.-H. Huo, S. Höfling, C.-Y. Lu, and J.-W. Pan, Phys. Rev. Lett. **122**, 113602 (2019).
[18]A. Tribu, G. Sallen, T. Aichele, R. André, J.-P. Poizat, C. Bougerol, S. Tatarenko, and K. Kheng, Nano Lett. **8**, 4326 (2008).
[19]M. Arita, F. Le Roux, M. J. Holmes, S. Kako, and Y. Arakawa, Nano Lett. **17**, 2902 (2017).
[20]H. P. Springbett, K. Gao, J. Jarman, T. Zhu, M. Holmes, Y. Arakawa, and R. A. Oliver, Appl. Phys. Lett. **113**, 101107 (2018).
[21]J.-H. Cho, Y. M. Kim, S.-H. Lim, H.-S. Yeo, S. Kim, S.-H. Gong, and Y.-H. Cho, ACS Photonics **5**, 439 (2018).
[22]L. Zhang, C.-H. Teng, T. A. Hill, L.-K. Lee, P.-C. Ku, and H. Deng, Appl. Phys. Lett. **103**, 192114 (2013).
[23]T. Jemsson, H. Machhadani, P.-O. Holtz, and K. F. Karlsson, Nanotechnology **26**, 065702 (2015).
[24]S. Kremling, C. Tessarek, H. Dartsch, S. Figge, S. Höfling, L. Worschech, C. Kruse, D. Hommel, and A. Forchel, Appl. Phys. Lett. **100**, 061115 (2012).
[25]M. Holmes, S. Kako, K. Choi, M. Arita, and Y. Arakawa, Phys. Rev. B **92**, 115447 (2015).
[26]R. A. Oliver, G. A. D. Briggs, M. J. Kappers, C. J. Humphreys, S. Yasin, J. H. Rice, J. D. Smith, and R. A. Taylor, Appl. Phys. Lett. **83**, 755 (2003).
[27]A. Woolf, T. Puchtler, I. Aharonovich, T. Zhu, N. Niu, D. Wang, R. Oliver, and E. L. Hu, Proc. Natl. Acad. Sci. U. S. A. **111**, 14042 (2014).
[28]K. Gao, H. Springbett, T. Zhu, R. A. Oliver, Y. Arakawa, and M. J. Holmes, Appl. Phys. Lett. **114**, 112109 (2019).
[29]F. C.-P. Massabuau, P. H. Griffin, H. P. Springbett, Y. Liu, R. V. Kumar, T. Zhu, and R. A. Oliver, APL Mater. **8**, 031115 (2020).
[30]F. C.-P. Massabuau, H. P. Springbett, G. Divitini, P. H. Griffin, T. Zhu, and R. A. Oliver, Materialia **12**, 100798 (2020).
[31]V. A. Fonoberov, E. P. Pokatilov, and A. A. Balandin, J. Nanosci. Nanotechnol. **3**, 253 (2003).
[32]M. Winkelnkemper, A. Schliwa, and D. Bimberg, Phys. Rev. B **74**, 155322 (2006).
[33]D. P. Williams, A. D. Andreev, and E. P. O'Reilly, Phys. Rev. B **73**, 241301 (2006).
[34]J. Iles-Smith, D. P. S. McCutcheon, A. Nazir, and J. Mørk, Nat. Photonics **11**, 521 (2017).
[35]P. Borri, W. Langbein, J. Mørk, J. M. Hvam, F. Heinrichsdorff, M.-H. Mao, and D. Bimberg, Phys. Rev. B **60**, 7784 (1999).
[36]A. Berthelot, I. Favero, G. Cassabois, C. Voisin, C. Delalande, P. Roussignol, R. Ferreira, and J. M. Gérard, Nat. Phys. **2**, 759 (2006).
[37]I. Favero, A. Berthelot, G. Cassabois, C. Voisin, C. Delalande, P. Roussignol, R. Ferreira, and J. M. Gérard, Phys. Rev. B **75**, 073308 (2007).
[38]I. A. Ostapenko, G. Hönig, S. Rodt, A. Schliwa, A. Hoffmann, D. Bimberg, M.-R. Dachner, M. Richter, A. Knorr, S. Kako, and Y. Arakawa, Phys. Rev. B **85**, 081303 (2012).
[39]R. Bardoux, T. Guillet, P. Lefebvre, T. Taliercio, T. Bretagnon, S. Rousset, B. Gil, and F. Semond, Phys. Rev. B **74**, 195319 (2006).
[40]S. Kako, M. Holmes, S. Sergent, M. Bürger, D. J. As, and Y. Arakawa, Appl. Phys. Lett. **104**, 011101 (2014).
[41]G. Sallen, A. Tribu, T. Aichele, R. André, L. Besombes, C. Bougerol, M. Richard, S. Tatarenko, K. Kheng, and J.-P. Poizat, Nat. Photonics **4**, 696 (2010).
[42]G. Sallen, A. Tribu, T. Aichele, R. André, L. Besombes, C. Bougerol, M. Richard, S. Tatarenko, K. Kheng, and J.-P. Poizat, Phys. Rev. B **84**, 041405 (2011).
[43]H. Wang, Y. He, Y.-H. Li, Z.-E. Su, B. Li, H.-L. Huang, X. Ding, M.-C. Chen, C. Liu, J. Qin, J.-P. Li, Y.-M. He, C. Schneider, M. Kamp, C.-Z. Peng, S. Höfling, C.-Y. Lu, and J.-W. Pan, Nat. Photonics **11**, 361 (2017).